

# Electrospray of an Energetic Ionic Liquid Monopropellant for Multi-Mode Micropropulsion Applications

Steven P. Berg<sup>1</sup> and Joshua L. Rovey<sup>2</sup>

*Missouri University of Science and Technology, Rolla, Missouri, 65409*

Benjamin D. Prince<sup>3</sup>, Shawn W. Miller<sup>4</sup> and Raymond J. Bemish<sup>5</sup>

*Air Force Research Laboratory, Kirtland AFB, Albuquerque, New Mexico, 87117*

The multi-mode chemical-electric propulsion capable energetic ionic liquid propellant [Emim][EtSO<sub>4</sub>]-HAN is electrosprayed in a 100  $\mu\text{m}$  capillary emitter to test the electric-mode performance of the propellant. The ionic liquid exhibits stable electrospray emission in both cation and anion extraction modes at a nominal extraction voltage of 3400 V. Near field measurements of current and mass flow rate distribution are taken at flow rates from 0.19 nL/s to 3.06 nL/s. Total emission current, as measured by Faraday cup and integrated, increases from 754 nA to 3195 nA for cation emission and from 552 nA to 2012 nA for anion emission. The thrust and specific impulse at 0.19 nL/s flow rate is 1.08  $\mu\text{N}$  and 412 seconds, respectively, with a beam power of 2.22 mW. At 3.06 nL/s, the thrust is 8.71  $\mu\text{N}$  and the specific impulse is 204 seconds with a beam power of 8.85 mW. Extrapolation of the current data shows that specific impulse in excess of 1000 seconds is achievable through optimized feed system and emitter design.

## Nomenclature

$D_c$	=	transport capillary inner diameter [ $\mu\text{m}$ ]
$D_n$	=	emitter inner diameter [ $\mu\text{m}$ ]
$F$	=	thrust [ $\mu\text{N}$ ]
$g_0$	=	constant to convert specific impulse to units of seconds [ $\text{m/s}^2$ ]
$I$	=	current [nA]
$I_{sp}$	=	specific impulse [sec]
$K$	=	ionic liquid electrical conductivity [S/m]
$L_c$	=	length of transport capillary [cm]
$L_n$	=	length of capillary emitter [cm]
$\dot{m}$	=	mass flow rate [ng/s]
$m/q$	=	mass to charge ratio [amu/e]
$P_0$	=	reservoir pressure [torr]
$P_c$	=	pressure in transport capillary [torr]
$P_n$	=	pressure at capillary emitter [torr]
$Q$	=	volumetric flow rate [nL/s]
$V_{acc}$	=	acceleration voltage [V]
$V_E$	=	extractor voltage [V]
$V_N$	=	emitter voltage [V]
$\gamma$	=	ionic liquid surface tension [N/m]

<sup>1</sup> Graduate Research Assistant, Aerospace Plasma Laboratory, Mechanical and Aerospace Engineering, 160 Toomey Hall, 400 W. 13<sup>th</sup> Street, Student Member AIAA.

<sup>2</sup> Associate Professor of Aerospace Engineering, Mechanical and Aerospace Engineering, 292D Toomey Hall, 400 W. 13<sup>th</sup> Street, AIAA Associate Fellow.

<sup>3</sup> Research Chemist, Space Vehicles Directorate, 3550 Aberdeen Ave SE. Bldg. 570, Member AIAA.

<sup>4</sup> Research Associate, Boston College, Institute for Scientific Research, 140 Commonwealth Ave., Member AIAA.

<sup>5</sup> Senior Research Chemist, Space Vehicles Directorate, 3550 Aberdeen Ave SE. Bldg. 570, Non-Member AIAA.

$\epsilon$	=	ionic liquid dielectric constant
$\epsilon_0$	=	permittivity of free space [F/m]
$\mu_l$	=	viscosity of propellant [cP]
$\rho$	=	ionic liquid density [g/cm <sup>3</sup> ]

## I. Introduction

**M**ULTI-mode spacecraft propulsion is the use of two or more types of propulsive devices on a spacecraft that share some commonality in terms of either hardware or propellant. An example is the Mars Global Surveyor, which made use of hydrazine as both a monopropellant for attitude control and a bipropellant for primary maneuvering.<sup>1</sup> Specific to this study is a multi-mode system making use of a high-thrust, usually chemical, mode and a high-specific impulse, electric mode. Using these two modes can be beneficial in two primary ways. One way is by designing a mission such that the high-thrust and high-specific impulse maneuvers are conducted in such a way that it provides a more optimum trajectory over a single chemical or single electric maneuver.<sup>2-5</sup> The second is to increase the mission flexibility of a single spacecraft architecture in that both high-thrust and high-specific impulse maneuvers are available to mission designers at will, perhaps even allowing for drastic changes in the mission plan while on-orbit or with a relatively short turnaround from concept to launch.<sup>6-10</sup> For the second method, it is extremely beneficial to utilize a common propellant for both modes as this provides the highest flexibility in terms of mission design choices.<sup>9</sup> Previous research has investigated a multi-mode system utilizing a single ionic liquid propellant for chemical monopropellant and electrospray modes.<sup>6,11</sup> Two propellants were developed that may not only function, but theoretically perform well in both a modes.<sup>11</sup> These propellants, based on binary mixtures of ionic liquid fuels [Emim][EtSO<sub>4</sub>] and [Bmim][NO<sub>3</sub>] with ionic liquid oxidizer hydroxylammonium nitrate (HAN), have been previously synthesized and tested for thermal and catalytic decomposition in a microreactor.<sup>12</sup> This paper presents results of experiments measuring the performance of the electrospray emitter and beam composition of the [Emim][EtSO<sub>4</sub>]-HAN propellant. In a separate paper, the decomposition and performance of this propellant in the chemical, high-thrust mode thruster has been investigated.<sup>13</sup>

Recent efforts have placed a greater emphasis on smaller spacecraft, specifically microsattellites (10-100 kg) and nanosatellites (1-10 kg), including the subset of cubesats.<sup>14</sup> Many different types of thrusters have been proposed to meet the stringent mass and volume requirements placed on spacecraft of this type. Electrospray, in particular, may be well suited for micropropulsion, and has been selected for these types of applications.<sup>15-17</sup> Several types of thrusters have been proposed for chemical propulsion for small spacecraft. One type is the chemical microtube.<sup>18-20</sup> This type of thruster is simply a heated tube of diameter ~1 mm or less that may or may not consist of a catalytic surface material. Additionally, and ideally from a multi-mode system standpoint, there is no fundamental reason why this geometry could not be shared with the electrospray mode as capillary type emitters can be roughly the same diameter tube.<sup>21</sup> This would reduce the overall propulsion system mass, which is desirable particularly in micropropulsion systems for small spacecraft.

Electrospray is a propulsion technology in which charged liquid droplets or ions are extracted from an emitter via an applied electric field. This produces a high exhaust velocity (high specific impulse) but low flow rate and thrust.<sup>16</sup> Ionic liquids are candidates for electrospray propulsion not only due to their ionic nature, but also their negligible vapor pressure and high electrical conductivity.<sup>22</sup> Charged species emitted from the ionic liquid can range from large m/q charged droplets to a purely ionic regime (PIR), with small m/q values, similar to that of field emission electric propulsion with specific impulses in the range of 200-4000 seconds for current propellants.<sup>16</sup> The ionic liquid 1-ethyl-3-methylimidazolium bis(trifluoromethylsulfonyl)imide ([Emim][Im], or [Emim][Tf<sub>2</sub>N]) was selected as the propellant for the ST7 Disturbance Reduction System mission, and represents the only planned flight application of electrospray, or colloid, thrusters to date.<sup>17</sup> Several other imidazole-based ionic liquids have been suggested for research in electrospray propulsion due to their favorable physical properties, however, none of these have energetic properties sufficient for chemical propulsion.<sup>17</sup>

Electrospray liquids with relatively high vapor pressure boil off the propellant and produce an uncontrolled, low performance emission. This virtually eliminates most of the advanced monopropellants from multi-mode propulsion consideration since although their main component is an ionic liquid oxidizer, they typically contain water and perhaps a volatile fuel component.<sup>23-25</sup> Mixing electrosprayable, fuel-rich ionic liquids with an ionic liquid oxidizer such as HAN shows theoretical promise in terms of achieving high performance in both chemical and electrospray modes.<sup>11</sup> However, it is difficult to theoretically predict electrospray performance precisely due to relative immaturity of the technology. Additionally, the double salt nature of the ionic liquid propellants to be investigated here could lead to additional difficulties in predicting the electrospray performance.<sup>26</sup> This will be discussed in further detail in a later section, but this illustrates the need for experimental measurements in order to best estimate

electrospray performance. This paper describes experimental measurements of the performance and beam properties of the electrospray emission of the double salt ionic liquid propellant [Emim][EtSO<sub>4</sub>]-HAN. Section II describes the experimental setup and propellant synthesis. Section III presents the results of the electrospray experiments. Section IV discusses the results and performance of the propellant in a capillary electrospray system. Section V summarizes the relevant conclusions.

## II. Experimental Setup

The electrospray thruster experiment utilized to characterize electrospray performance is a well-characterized experiment that is currently in use at AFRL Kirtland<sup>27,28</sup>. The experiment consists of a capillary emitter electrospray source, which is effectively the same geometry as the chemical thruster microtube, Figure 1a,<sup>13</sup> but with a voltage applied between the needle tip and an extractor grid, Figure 1b. In order to characterize the performance of the electrospray emission mode, knowledge of the beam current and mass flow rate is required. These measurements are accomplished using the angle-resolved method described by Chiu, et. al.<sup>28</sup> and also conducted by Miller, et.al.<sup>27</sup> to study the capillary electrospray of the ionic liquid [Bmim][dca].

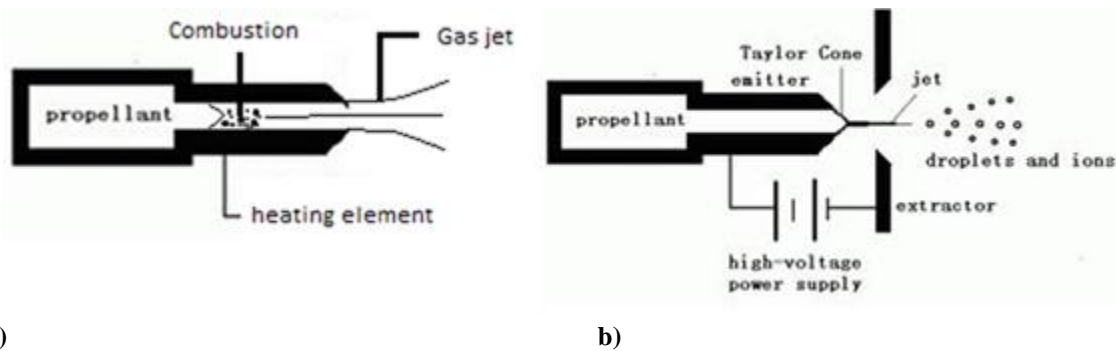


**Figure 1. Multi-mode thruster operated in a) chemical microtube and b) electrospray emission modes.**

### A. Apparatus

A schematic of the instrumentation to diagnose the electrospray emission in the near-field is shown in Figure 2. The electrospray source, as in Figure 1b, consists of a capillary and extractor plate. The capillary is 100  $\mu\text{m}$  internal diameter, 5.0 cm long, and has a tapered tip. The capillary is fed from a propellant reservoir via a 100  $\mu\text{m}$  internal diameter fused silica transport capillary 82.5 cm in length. The feed system is a pressure-fed system similar to that used by Lozano<sup>29</sup> and is shown in Figure 3. Notable differences include direct feed pressure monitoring via a pressure transducer and the fact the reservoir, after achieving nominal pressure, is isolated by closing both shut-off valves and operates in blow-down mode. Since the volume change of the propellant in the reservoir is negligible during normal test operations ( $\sim\text{nL/s}$  flow rate from a  $\sim 10$  mL reservoir), reservoir pressure, and thus flow rate, can safely be assumed to be constant during the experiment under steady flow conditions. The extractor plate consists of a metal plate with a 1.5 mm orifice to allow for passage of the electrospray beam.

The electrospray source is attached to a rotation stage, which allows the beam to be rotated in order to capture species in the full width of the beam divergence. These measurements allow for computation of the thrust, specific impulse, and efficiency of the electrospray thruster. A Faraday cup and quartz crystal microbalance (QCM) measure the current and mass flow rate of the electrospray beam. Apparatuses of 0.8 mm are used on both targets located 18 mm downstream of the emission source, and the measurement interval is at minimum 2.5 degrees for all angle-resolved measurements described in this paper.

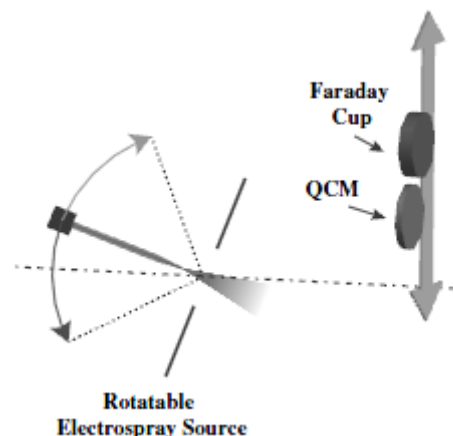


**Figure 2. Electro spray experiment near-field diagnostics.**<sup>27,28</sup>

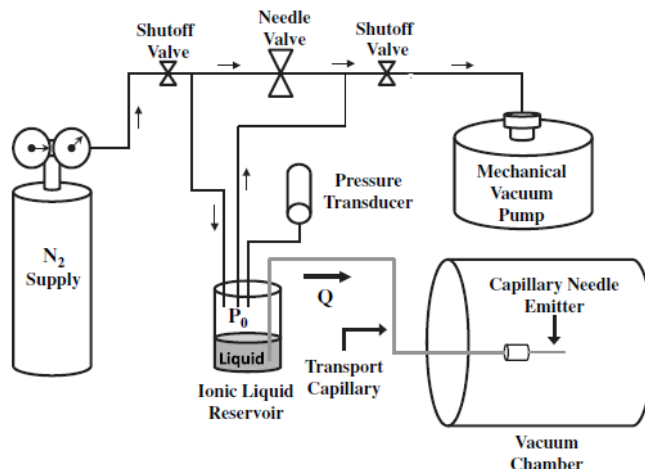


Figure 3. Plumbing and instrumentation diagram of the electro spray apparatus.<sup>27</sup>

While the experiment itself is well characterized with various ionic liquids, there are notable differences between ionic liquids previously investigated with the setup and the ionic liquid propellants proposed in this study. The major difference is that previously only single ionic liquids have been used. The multi-mode propellants proposed here are mixtures of two ionic liquids. Furthermore, the term mixture is actually a misnomer and these may in fact be more accurately referred to as double salt ionic liquids<sup>26</sup>. The reason is in the fundamental nature of ionic liquids, in that they are essentially dissociated pairs of cations and anions in solution. Therefore mixing two ionic liquids could result in not only pairs of the original constituents, but also pairs of the swapped ions. For example, a mixture of two ionic liquids  $[A]^+[B]^-$  and  $[C]^+[D]^-$  could consist of a mixture of  $[A]^+[B]^-$ ,  $[C]^+[D]^-$ ,  $[A]^+[D]^-$ ,  $[C]^+[B]^-$  in some ratio. While trends in the literature predict that the physical properties for double salt ionic liquids in general follow typical mixing laws<sup>26</sup>, this could fundamentally alter the species emitted in the electro spray beam, and thus have an effect on the electro spray thruster performance of the ionic liquid propellants.

### B. Propellant Synthesis

The propellant synthesis method for the binary mixture of  $[Emim][EtSO_4]$ -HAN was developed in a previous study,<sup>12</sup> however it is repeated here making particular note of the considerations made to ensure successful electro spray operation. Pure 1-ethyl-3-methylimidazolium ethyl sulfate,  $[Emim][EtSO_4]$  (95% purity), and hydroxylammonium nitrate, HAN, (24% in water) were purchased from Sigma Aldrich. Pure crystalline HAN was obtained by removing water in high-vacuum ( $\sim 10^{-6}$  torr) for  $\sim 8$  h. Additionally,  $[Emim][EtSO_4]$  was placed in high vacuum for  $\sim 8$ h to remove any volatile impurities. Crystalline HAN was then added to the  $[Emim][EtSO_4]$  in a sealable container in the desired ratio; for this study the ratio is 59% HAN, 41%  $[Emim][EtSO_4]$  by weight. This ratio was chosen mostly to avoid sooting and burn through in the chemical mode and is described more in the previous studies with this propellant.<sup>11,12</sup> This mixture was allowed to settle overnight at which point solid HAN was no longer visible in the mixture. This process likely could be sped up by mechanically agitating the mixture to allow for faster dissolving. However, due to safety concerns involved with creating the potentially explosive monopropellant, this was avoided, and is not recommended. The propellant reservoir in the electro spray experiment described in this paper was kept under rough vacuum ( $< 100$  mTorr) when not in operation to prevent water absorption.

### III. Results

The following section presents results from the near field experiment which measures current and flow rate distribution as a function of angle of the electro spray beam in the region of  $\pm 60$  degrees in reference to the center of the beam. These measurements will be used to calculate emitter performance in the next section. All measurements in this section are taken with an extraction voltage of 3400 V for both cation ( $V_N = +900$  V,  $V_E = -2500$  V) and anion ( $V_N = -900$  V,  $V_E = +2500$  V) emission. This was found to be the nominal extraction voltage through trial and error, providing a stable beam.

### A. Flow Rate Calibration-Bubble Method

Flow rate is primarily calibrated using the bubble method, and flow rates in the remainder of this paper, except where noted, refer to the values determined through this method. For this method, a bubble is introduced to the transport capillary at its termination in the reservoir. Since the capillary is made of transparent material, the bubble movement can be tracked visually via the use of a magnifying glass. Flow rate as a function of reservoir pressure can then be determined by measuring the distance the bubble travels as a function of time, as measured by a stop watch. The total duration of each test was kept longer than ~15 sec to minimize error from a slow trigger finger. Results are shown in Figure 4. Additionally, the experimental results can be compared to analytical calculations given by the Hagan-Poiseuille equation, Eq. (1),

$$Q = \frac{\pi D_c^4}{128\mu_l} \frac{(P_0 - P_n)}{L_c} = \frac{\pi D_n^4}{128\mu_l} \frac{(P_n - P_c)}{L_n} \quad (1)$$

where the length and diameter of the capillary and transport capillary are given in the previous section and the viscosity of the liquid propellant is 130 cP as found in a previous experiment.<sup>13</sup> The flow rate range achieved by the feed system is similar to that conducted for electrospray [Bmim][dca] in a capillary emitter.<sup>27</sup> However, the emitter diameter for the [Bmim][dca] experiments was half that of the current experiments. The flow rate similarity is due to the fact that the viscosity of the [Emim][EtSO<sub>4</sub>]-HAN propellant is roughly four times that of [Bmim][dca].

### B. Angle-Resolved Current Measurements

Beam current measurements as a function of emitter angle to the Faraday cup are taken for both cation and anion emission at the aforementioned extraction conditions and for the range of flow rates illustrated in Figure 4. Total current is calculated by integrating the associated current density profile over a hemisphere, similar to the analysis for a Hall thruster plume conducted by Manzella and Sankovic<sup>30</sup> and the same analysis conducted by Miller, et. al.<sup>27</sup> Additionally, total emission current on the needle and loss to the extractor is monitored by measuring the potential across a 4.93 MΩ resistor on the associated voltage line for comparison to and verification of the integrated results.

Current density profiles for various flow rates are shown for the electrospray emission in Figure 5. Figure 5a shows the cation emission profile. The highest current densities are obtained near the centerline for each flow rate and decrease as flow rate is increased, peaking at 3.1 nA/mm<sup>2</sup> for 0.19 nL/s and 2.4 nA/mm<sup>2</sup> for 3.06 nL/s. The beam width grows as flow rate is increased, from a 70 degrees at 0.19 nL/s to nearly 90 degrees at 3.09 nL/s, and is roughly 5 degrees asymmetric toward the positive angles. Profiles for anion emission are similar, and are shown in Figure 5b. Peak current is slightly higher for the anion emission compared to the cation emission, with the current density reaching 3.3 nA/mm<sup>2</sup> for 0.19 nL/s flow rate and decreasing to 2.8 nA/mm<sup>2</sup> for 3.06 nL/s flow rate. The beam is slightly narrower compared to the cation case. The beam has a width of 60 degrees for 0.19 nL/s flow rate and increases to 75 degrees for 3.06 nL/s flow rate.

Total emission current obtained by integrating the beam current profiles, along with the measurements from the 4.93 MΩ resistor are shown in Figure 6. The integrated current is the total current obtained by integrating the current profiles in Figure 5 via the method described previously. The emitter current is measured on the needle and is a measure of the overall total current of the electrospray emission. The extractor current is the current lost to the extractor. Figure 6a shows the results from cation emission. At the lowest flow rate conducted in the experiment, 0.19 nL/s, the total current is 680 nA. Both the integrated and emitter current agree at low flow rates. However, due to loss to the extractor at higher flow rates, the current measured via integration of the Faraday cup measurements does not increase markedly although the emitter current does. At the highest flow rate at which experiments were conducted, 3.1 nL/s, the loss to the extractor represents nearly 2/3 of the total emission current. Current measured for anion emission is shown in Figure 6b. The trends in total current are similar to the cation case; however, the current at each flow rate is roughly 70% that of the cation case. The current integrated from the angle-resolved

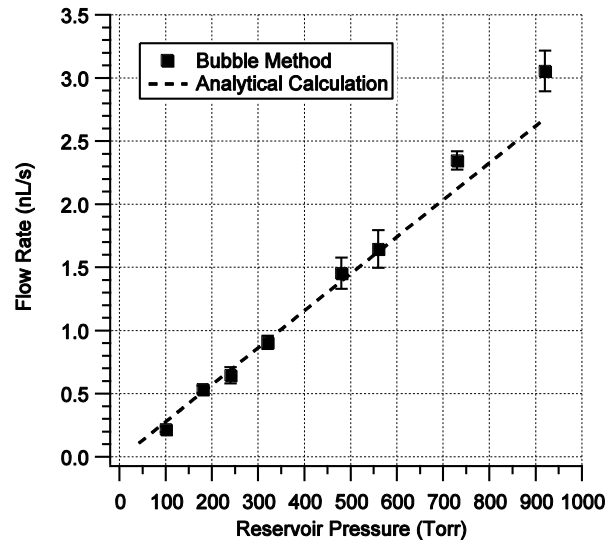


Figure 4. Flow rate as a function of reservoir pressure obtained via the bubble method.

profiles added to the current measured on the extractor agrees well with the emitter current, within 15% for all flow rate cases.

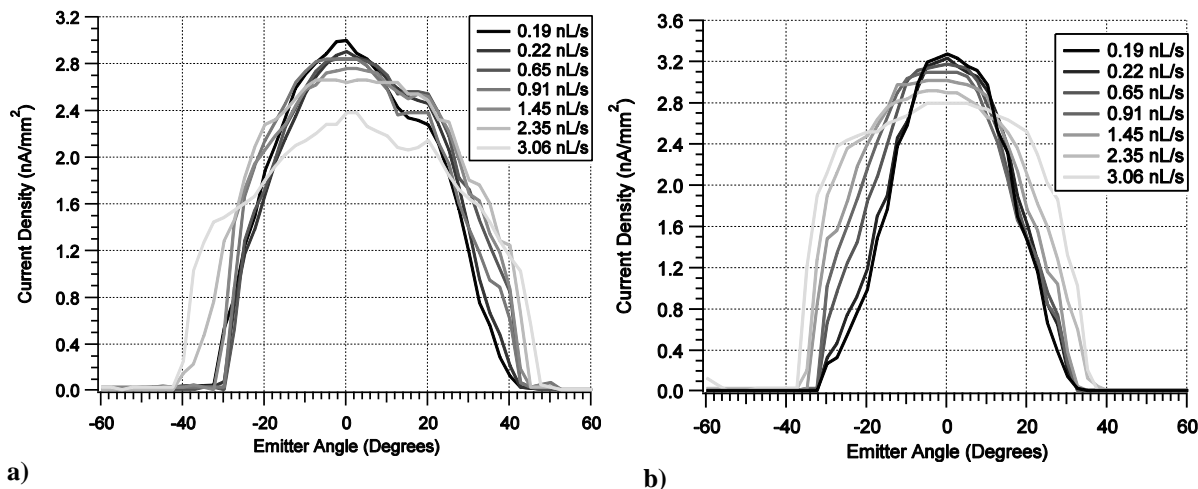


Figure 5. Current density profiles for a) cation and b) anion emission of the electrospray of [Emim][EtSO<sub>4</sub>]-HAN propellant.

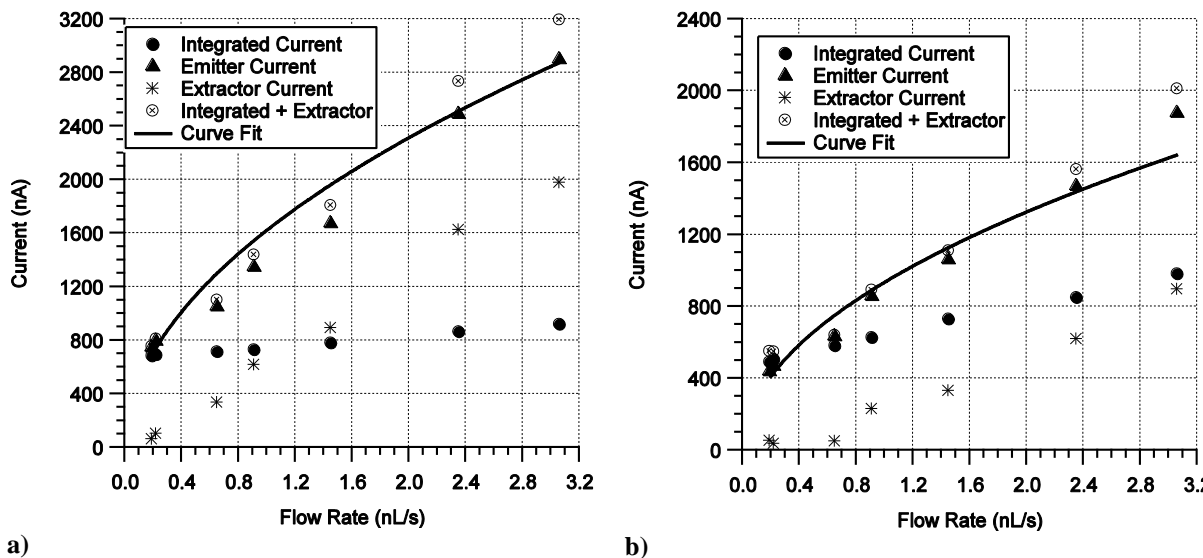


Figure 6. Total emission current as a function of propellant flow rate for a) cation and b) anion emission.

### C. Angle-Resolved Mass Flow Measurements

Mass flux as a function of emitter angle is measured in a similar manner to the current profiles with the QCM, but for flow rates from 0.19 nL/s to 1.45 nL/s. Higher flow rates are omitted since the nature of the QCM prevents reliable measurements at higher flow rates. The situation is described in more detail in the work by Miller, et. al.,<sup>27</sup> but is essentially due to violation of the thin film assumption resulting from accumulation of the ionic liquid on the QCM, which does not boil off due to the negligible vapor pressure of the ionic liquid. Raw output of the QCM is converted to mass flux by using the measured density of the ionic liquid propellant (1.42 g/cm<sup>3</sup>)<sup>12,13</sup> and includes small aperture and area ratio corrections.<sup>31</sup>

The mass flux profile for both cation and anion emission as a function of angle is shown in Figure 7. Cation emission is shown in Figure 7a. Peak mass flux, as with current density, occurs at or near the centerline. The peak

mass flux for the 0.19 nL/s case is 1.3 ng/s-mm<sup>2</sup> and for the 1.45 nL/s case is 4.5 ng/s-mm<sup>2</sup>. The first instance of non-zero mass flux is seen at -25 degrees emitter angle for all flow rates. This is somewhat notable as non-zero current is seen at -30 degrees, as presented in Figure 5. The same trends are seen for anion emission, as shown in Figure 7b, and in fact the profiles are virtually identical numerically by visual inspection.

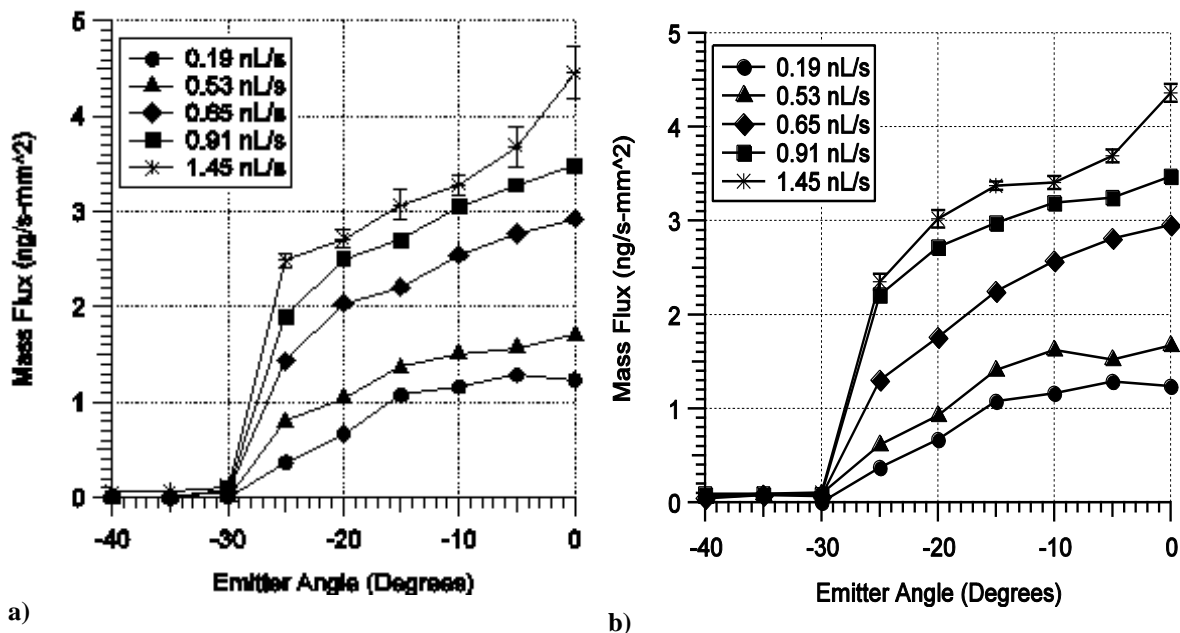


Figure 7. Mass flux profiles for emission of a) cations and b) anions.

The mass flux profiles are integrated over a hemisphere in the same manner as described in the total current integration. Results of the integration are shown in Table 1 and compared to the nominal mass flow rate measured by the bubble method. As with the current measurements, the integrated mass flow rate agrees with the nominal mass flow rate at low flow rates. However, this quickly diverges as flow rate is increased. At the highest flow rate, 1.45 nL/s, integration of measurements taken via the QCM results in a roughly 50% reduced flow rate value. Also notable is that, except for the 0.22 nL/s case, the mass flow rate obtained via integration of the QCM data is smaller than that of the mass flow rate measured by the bubble method.

Table 1. Mass flow rate integrated from QCM data compared to bubble method.

Flow Rate (nL/s)	Integrated Mass Flow (ng/s)	Nominal Mass Flow (ng/s)	% Difference
<i>Cation Emission</i>			
0.19	268	269	0.51
0.22	334	312	-7.27
0.65	720	922	21.89
0.91	890	1291	31.08
1.45	1012	2057	50.82
<i>Anion Emission</i>			
0.19	265	269	1.39
0.22	394	312	26.34
0.65	679	922	26.33
0.91	967	1291	25.10
1.45	1065	2057	48.24

## IV. Discussion

The near-field measurements described in the previous section provide information on the current and mass distribution of the electro spray emission of the double-salt ionic liquid propellant. Integration of the results from these measurements can be used to predict the performance characteristics of the ionic liquid propellant in an electro spray thruster. While the experiments conducted in this study do not represent the entirety of the possible performance envelope of the propellant, results can be extrapolated to determine the likely bounds of performance for this propellant.

### A. Current and Mass Distributions

The current and mass distributions of the electro spray of the [Emim][EtSO<sub>4</sub>]-HAN double-salt ionic liquid propellant follow trends seen in the literature.<sup>27</sup> Namely, the peak current falls as flow rate is increased and the profile becomes wider, resulting in a higher total integrated current. As noted in the previous section, the QCM data shows a non-zero flow rate at roughly 5 degrees closer to centerline than does the current. This supports the conclusion that much of the species comprising the outer portions of the beam are ions, whereas the center contains higher mass droplets. The mass flow of the ions is so small that it would not read a significant amount on the QCM.

Integrating the current data from the Faraday cup measurements and comparing to the current obtained from measuring the voltage across a resistor on the emitter and extractor lines shows that losses to the extractor become large as flow rate is increased. As mentioned, at the highest flow rates conducted in this study the loss is as much as 66% of the total emission current. This can likely be mitigated with an extractor designed and optimized for this propellant specifically; however, as will be shown in the next sub-section, these flow rates do not represent conditions in which a thruster would likely be operated. Adding the current obtained from the extractor resistor to the integrated current shows good agreement with the current obtained from the emitter resistor measurements, with most values falling within roughly 15% of each other. Though not shown in Figure 6, the measurement error for the resistor currents was also roughly 15%. This represented the average of the highest and lowest values observed on a digital readout, since these values were not instantaneously averaged via computer software but rather recorded by hand. Thus, the error also likely represents higher than one standard deviation.

As in the study of capillary electro spray emission of [Bmim][dca],<sup>27</sup> total mass flow rate calculated by integration of QCM data results agrees well with that obtained by the bubble method at low flow rates, but diverges as flow rate is increased. Curiously, in this study the mass flow calculated by QCM integration is lower than that of the bubble method, whereas in the [Bmim][dca] study it was higher. During the unfortunate situation in which a large amount of liquid was unintentionally deposited on the outer surface of the capillary, the propellant was actually observed to boil in the high vacuum conditions ( $\sim 10^{-6}$  torr). This is likely the HAN component of the propellant. As a result, liquid deposited on the QCM in any significant amount would contribute a negative component to the mass flow rate during testing operations and would explain why the integrated mass flow rate is lower than the mass flow obtained by the bubble method.

### B. Performance

The primary goal of this study is to predict thruster performance of the [Emim][EtSO<sub>4</sub>]-HAN propellant operating in the electro spray mode of the proposed multi-mode system. The current and mass flow measurements obtained experimentally are directly used to compute performance. Thrust is calculated by Eq. (2),

$$F = \sqrt{2V_{acc}\dot{m}I} \quad (2)$$

where the current used is the integrated current profile plus extractor current shown in Figure 6. Although the extractor current does not contribute to actual thrust in this experiment, it still represents thrust that could be achieved through optimized extractor design. The specific impulse is then, Eq. (3),

$$I_{sp} = \frac{F}{\dot{m}g_0} \quad (3)$$

Current and calculated thrust values are shown in Table 2 for both cation and anion emission separately. Thrust for both cases is on the order of  $\mu\text{N}$  for this single emitter case. The thrust at the lowest flow rate is  $\sim 1 \mu\text{N}$  and increases to  $9.71 \mu\text{N}$  and  $7.71 \mu\text{N}$  for the cation and anion cases, respectively, at the highest tested flow rate of  $3.06 \text{ nL/s}$ .



Thrust is roughly 17% lower for anion emission compared to cation emission, a direct result of the lower current generated by the anion beam.

**Table 2. Current, thrust, and mass to charge ratio for cation and anion emission.**

Flow Rate (nL/s)	Mass Flow (ng/s)	Current (nA)	Thrust ( $\mu$ N)	m/q (amu)
<i>Cation Emission</i>				
0.19	269	754	1.18	34508
0.22	312	811	1.31	37137
0.65	922	1101	2.63	80815
0.91	1291	1439	3.56	86579
1.45	2057	1807	5.03	109860
2.35	3334	2733	7.87	117722
3.06	4342	3194	9.71	131170
<i>Anion Emission</i>				
0.19	269	551	1.01	47170
0.22	312	547	1.08	55022
0.65	922	640	2.00	139028
0.91	1291	891	2.80	139769
1.45	2057	1110	3.94	178742
2.35	3334	1562	5.95	206000
3.06	4342	2011	7.71	208281

An actual thruster would likely not operate in solely cation or anion emission mode, but rather in AC mode to prevent charge build up and eventual fouling of the emitter. Thus, in order to gauge performance, both the cation and anion emission must be taken into account. Table 3 shows the average thrust of the cation and anion emission at the tested flow rates, along with the beam power and specific impulse. Power ranges from 2.22 mW at the 0.19 nL/s flow rate to 8.85 mW for the 3.06 nL/s flow rate. Thrust per power (in  $\mu$ N/mW), however, at low flow rate is roughly 0.5 and improves to roughly 1.0 at high flow rate. Specific impulse decreases as flow rate increases, with a calculated value of 412.37 seconds at 0.19 nL/s flow rate and 204.47 seconds at 3.06 nL/s. These values are higher than the specific impulse predicted for the chemical propulsion mode (~180 seconds).<sup>13</sup>

**Table 3. Thrust, power, and specific impulse for electrospray emission.**

Flow Rate (nL/s)	Mass Flow (ng/s)	Average Thrust ( $\mu$ N)	Power (mW)	Isp (sec)
0.19	269	1.09	2.22	412
0.22	312	1.20	2.31	390
0.65	922	2.32	2.96	255
0.91	1291	3.18	3.96	250
1.45	2057	4.49	4.96	222
2.35	3334	6.91	7.30	211
3.06	4342	8.71	8.85	204

Although the highest specific impulse measured in this study is 412 seconds, this number could likely be improved through optimized thruster and feed system design. In order to gauge what might be possible, scaling laws

can be used to extrapolate the data garnered in this study to possible specific impulse and thrust values. Current in the mixed ion-droplet regime typically scales with flow rate as a power function according to Eq. (4),

$$I(Q) = f(\varepsilon) * \left[ \frac{\gamma K Q}{\varepsilon} \right]^{0.5} \quad (4)$$

Applying a curve fit to the beam current, shown in Figure 6, yields an exponent of approximately 0.5 (0.5092 for cation emission and 0.5019 for anion emission.), with coefficients of 1629.7 and 939.41 for cation and anion emission, respectively. The average of these two values, along with Eqs. (2) and (3) is used to calculate the thrust and specific impulse as a function of flow rate for a range of flows from 0.001 nL/s to 1 nL/s, shown in Figure 8. Achieving a lower flow rate results in a large increase in specific impulse. For the range in the figure, a specific impulse of 1000 seconds is possible if the flow rate could be reduced to 0.001 nL/s. For stable electro spray emission, the flow rate cannot be arbitrarily small and can be predicted through knowledge of the physical properties of the ionic liquid, Eq. (5),

$$Q_{min} = \frac{\gamma \varepsilon \varepsilon_0}{\rho K} \quad (5)$$

Although the surface tension, electrical conductivity, and dielectric constant of this propellant are not currently known, the value calculated for minimum flow of [Bmim][dca] was 0.09 pL/sec,<sup>27</sup> much lower than the 1 pL/sec shown in Figure 8. Thus, it is likely that performance is not limited by electro spray physics, but rather feed system performance in relation to the thruster geometry. Improvements in the feed system and optimization of emitter geometry for this propellant are likely to result in much improved performance in terms of specific impulse.

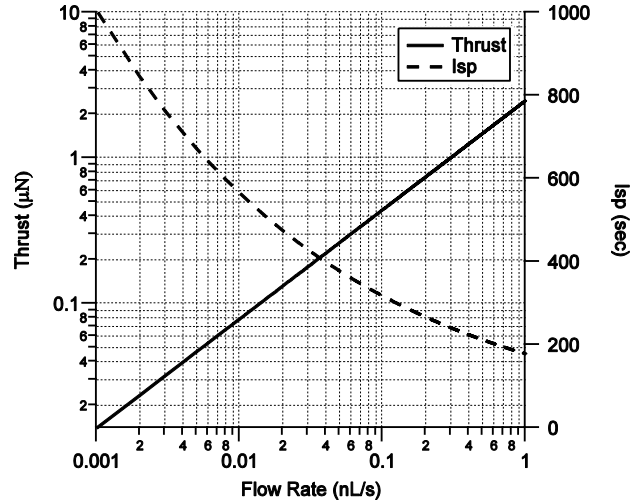


Figure 8. Thrust and specific impulse of IL propellant in a capillary emitter extrapolated from experimental data.

## V. Conclusions

The double-salt, energetic ionic liquid propellant [Emim][EtSO<sub>4</sub>]-HAN exhibits stable electro spray emission of both cations and anions in a capillary emitter of 100 μm inner diameter with a nominal extraction voltage of 3400 V. Near-field measurements of current and mass flow rate distribution exhibit trends similar to those of other propellants in the literature. The peak current, in the center of the beam, decreases with increase in mass flow rate, however the beam becomes wider and thus total integrated current increases. Current loss to the extractor increases with increasing flow rate, but could be mitigated with an extractor design optimized specifically for this propellant.

The lowest flow rate achieved in this experiment was 0.19 nL/s. This corresponds to the highest specific impulse achieved in this experiment, 412.37 seconds. The thrust at this specific impulse was calculated to be 1.09 μN, and higher thrust is possible with higher flow rates. At the highest flow rate tested, the thrust was 8.71 μN, which also corresponds to the highest thrust per unit power achieved in these experiments. Extrapolation of the data obtained from the electro spray emission currents shows that higher performance, in terms of specific impulse is possible. For example, if 1 pL/s flow rate could be achieved, the specific impulse would be 1000 seconds. Examination of the scaling laws for minimum flow rate reveals that the electro spray physics likely do not prohibit this performance from being achieved. It is therefore likely that improvements to the feed system and optimization of the emitter hardware in reference to this propellant specifically can realize higher performance than achieved in these experiments.

## References

- <sup>1</sup>Dominick, S., "Design, Development, and Flight Performance of the Mars Global Surveyor Propulsion System," *35th AIAA Joint Propulsion Conference*, AIAA Paper 1999-2176, 1999.
- <sup>2</sup>Kluever, C. A., "Spacecraft Optimization with Combined Chemical-Electric Propulsion," *Journal of Spacecraft and Rockets*, Vol. 32, No. 2, 1994, pp. 378-380.
- <sup>3</sup>Kluever, C. A., "Optimal Geostationary Orbit Transfers Using Onboard Chemical-Electric Propulsion," *Journal of Spacecraft and Rockets*, Vol. 49, No. 6, 2012, pp. 1174-1182.
- <sup>4</sup>Oh, D. Y., Randolph, T., Kimbrel, S., and Martinez-Sanchez, M., "End-to-End Optimization of Chemical-Electric Orbit Raising Missions," *Journal of Spacecraft and Rockets*, Vol. 41, No. 5, 2004, pp. 831-839.
- <sup>5</sup>Oleson, S. R., Myers, R. M., Kluever, C. A., Riehl, J. P., Curran, F. M., "Advanced Propulsion for Geostationary Orbit Insertion and North-South Station Keeping," *Journal of Spacecraft and Rockets*, Vol. 34, No. 1, 1997, pp. 22-28.
- <sup>6</sup>Donius, B. R. and Rovey, J. L., "Ionic Liquid Dual-Mode Spacecraft Propulsion Assessment," *Journal of Spacecraft and Rockets*, Vol. 48, No. 1, 2011, pp. 110-123.
- <sup>7</sup>Rexius, T., and Holmes, M., "Mission Capability Gains from Multi-Mode Propulsion Thrust Profile Variations for a Plane Change Maneuver," *AIAA Modeling and Simulation Technologies Conference*, AIAA Paper 2011-6431, 2011.
- <sup>8</sup>Haas, J. M., and Holmes, M. R., "Multi-Mode Propulsion System for the Expansion of Small Satellite Capabilities," NATO, Rept. MP-AVT-171-05, 2010.
- <sup>9</sup>Berg, S. P., and Rovey, J. L., "Assessment of Multi-Mode Spacecraft Micropropulsion Systems," *50th AIAA/ASME/SAE/ASEE Joint Propulsion Conference*, AIAA Paper 2014-3758, 2014.
- <sup>10</sup>Berg, S. P., and Rovey, J. L., "Assessment of High-Power Electric Multi-Mode Spacecraft Propulsion Concepts," *33rd International Electric Propulsion Conference*, IEPC-2013-308, 2013.
- <sup>11</sup>Berg, S. P., and Rovey, J. L., "Assessment of Imidazole-Based Energetic Ionic Liquids as Dual-Mode Spacecraft Propellants," *Journal of Propulsion and Power*, Vol. 29, No. 2, 2013, pp. 339-351.
- <sup>12</sup>Berg, S. P., and Rovey, J. L., "Decomposition of Monopropellant Blends of Hydroxylammonium Nitrate and Imidazole-Based Ionic Liquid Fuels," *Journal of Propulsion and Power*, Vol. 29, No. 1, 2013, pp. 125-135.
- <sup>13</sup>Berg, S. P., and Rovey, J. L., "Ignition and Performance of Ionic Liquid Propellants in a Microtube for Multi-Mode Micropropulsion Applications," *51st AIAA/ASME/SAE/ASEE Joint Propulsion Conference*, to be presented, 2015.
- <sup>14</sup>Green Monopropellant Thrusters, [http://www.busek.com/index\\_htm\\_files/70008517B.pdf](http://www.busek.com/index_htm_files/70008517B.pdf)
- <sup>15</sup>Busek Electro Spray Thrusters, [http://www.busek.com/index\\_htm\\_files/70008500E.pdf](http://www.busek.com/index_htm_files/70008500E.pdf)
- <sup>16</sup>Chiu, Y., Dressler, A., "Ionic Liquids For Space Propulsion", *Ionic Liquids IV: Not Just Solvents Anymore*, Vol. 975, American Chemical Society, Washington, D. C., 2007, Ch.
- <sup>17</sup>Gamero-Castano, M., "Characterization of a Six-Emitter Colloid Thruster Using a Torsional Balance," *Journal of Propulsion and Power*, Vol. 20, No. 4, 2004, pp. 736-741.
- <sup>18</sup>Mento, C. A., Sung, C-J., Ibarreta, A. F., Schneider, S. J., "Catalyzed Ignition of Using Methane/Hydrogen Fuel in a Microtube for Microthruster Applications," *Journal of Propulsion and Power*, Vol. 25, No. 6, 2009, pp. 1203-1210.
- <sup>19</sup>Boyarko, G. A., Sung, C-J., Schneider, S. J., "Catalyzed Combustion of Hydrogen-Oxygen in Platinum Tubes for Micropropulsion Applications," *Proceedings of the Combustion Institute*, Vol. 30, No. 2005, pp. 2481-2488.
- <sup>20</sup>Volchko, S. J., Sung, C-J., Huang, Y., Schneider, S. J., "Catalytic Combustion of Rich Methane/Oxygen Mixtures for Micropropulsion Applications," *Journal of Propulsion and Power*, Vol. 22, No. 3, 2006, pp. 684-693.
- <sup>21</sup>Alexander, M. S., Stark, J., Smith, K. L., Stevens, B., Kent, B., "Electrospray Performance of Microfabricated Colloid Thruster Arrays," *Journal of Propulsion and Power*, Vol. 22, No. 3, 2006, pp. 620-627.
- <sup>22</sup>Romero-Sanz, I., Bocanegra, R., Fernandez De La Mora, J., Gamero-Castano, M., "Source of Heavy Molecular Ions Based on Taylor Cones of Ionic Liquids Operating in the Pure Ion Evaporation Regime," *Journal of Applied Physics*, Vol. 94, No. 2003, pp. 3599-3605.
- <sup>23</sup>Amariei, D., Courtheoux, L., Rossignol, S., Batonneau, Y., Kappenstein, C., Ford, M., and Pillet, N., "Influence of the Fuel on Thermal and Catalytic Decompositions of Ionic Liquid Monopropellants," *41st AIAA/ASME/SAE/ASEE Joint Propulsion Conference & Exhibit*, AIAA Paper 2005-3980, 2005.
- <sup>24</sup>Anflo, K., Gronland, T. A., Bergman, G., Johansson, M., and Nedar, R., "Towards Green Propulsion for Spacecraft with ADN-Based Monopropellants," *38th AIAA/ASME/SAE/ASEE Joint Propulsion Conference & Exhibit*, AIAA Paper 2002-3847, 2002.
- <sup>25</sup>McLean, C. H., Deininger, W. D., Joniatis, J., Aggarwal, P. K., Spores, R. A., Deans, M., Yim, J. T., Bury, K., Martinez, J., Cardiff, E. H., Bacha, C. E., "Green Propellant Infusion Mission Program Development and Technology Maturation," *50th AIAA/ASME/SAE/ASEE Joint Propulsion Conference*, AIAA Paper 2014-3481, 2014.
- <sup>26</sup>Chatel, G., Pereira, J.F.B., Debbeti, V., Wang, H., Rogers, R.D., "Mixing Ionic Liquids-"Simple Mixtures" or "Double Salts"?, *Green Chemistry*, Vol. 16, No. 2014, pp. 2051-2083.
- <sup>27</sup>Miller, S.W., Prince, B.D., Bemish, R.J., Rovey, J.L., "Electrospray of 1-Butyl-3-Methylimidazolium Dicyanamide Under Variable Flow Rate Operations," *Journal of Propulsion and Power*, Vol. 30, No. 6, 2014, pp. 1701-1710.
- <sup>28</sup>Chiu, Y., Gaeta, G., Levandier, D.J., Dressler, R.A., Boatz, J.A., "Vacuum Electro Spray Ionization Study of the Ionic Liquid, [Emim][Im]," *International Journal of Mass Spectrometry*, Vol. 265, No. 2-3, 2007, pp. 146-158.
- <sup>29</sup>Lozano, P.C., "Studies on the Ion-Droplet Mixed Regime in Colloid Thrusters," 2003.

- <sup>30</sup>Manzella, D. H., and Sankovic, J. M., "Hall Thruster Ion Beam Characterization," *31st AIAA/ASME/ASEE Joint Propulsion Conference and Exhibit*, AIAA Paper 1995-2927, 1995.
- <sup>31</sup>Martin, B. A., and Hager, H. E. , "Velocity Profile on Quartz Crystals Oscillating in Liquids," *Journal of Applied Physics*, Vol. 65, No. 7, 1989, pp. 2630-2635.